RSC Advances

PAPER

View Article Online
View Journal | View Issue

Cite this: *RSC Adv.*, 2021, **11**, 38862

A top-down design for easy gram scale synthesis of melem nano rectangular prisms with improved surface area†

Mahsa Nikookar, [a] Abdolreza Rezaeifard, *[a] Maasoumeh Jafarpour, *[a] Kirill V. Grzhegorzhevskii [b] and Alexander A. Ostroushko [b]

Received 7th October 2021
Accepted 24th November 2021

DOI: 10.1039/d1ra07440g

rsc.li/rsc-advances

An unprecedented top-down design for the preparation of melem by 1 h stirring of melamine-based g-C_3N_4 in 80 °C concentrated sulfuric acid (95–98%) was discovered. The melem product was formed selectively as a monomer on the gram scale without the need for controlled conditions, inert atmosphere, and a special purification technique. The as-prepared air-stable melem showed a distinctive nano rectangular prism morphology that possesses a larger surface area than the melems achieved by traditional bottom-up designs making it a promising candidate for catalysis and adsorption processes.

Triamino-*s*-heptazine or 2,5,8-triamino-tri-*s*-triazine known as "melem", is a mysterious molecule and invaluable intermediate in the density of melamine rings to graphitic carbon nitride (g-C_3N_4) with a rigid heptazine structure with three pendant amino substituents.[1] Melem does not bear two of the strongest emission quenchers, namely C–H and O–H groups;[2] In this way it has unique optical properties[3] and is known as an efficient metal-free luminescent material.[4] High stability, the possibility for supramolecular self-assembly, tunable band gap, and an already rich physicochemical chemistry are some of the known properties for melem.[1b] For this reason, melem has the potential to be used in photocatalysts, MOFs, COFs, electrochemistry sensors, flame retardants, TADF and related OLEDs, and liquid crystals.[1] The use of melem in solar hydrogen evolution[5] and bioimaging[6] is also known.

Very few reports of its catalytic application are available, nevertheless, in recent years it has attracted much attention because of exploring its unique properties. Metal-free g-C_3N_4/melem hybrid photocatalysts have been used for visible-light-driven hydrogen evolution.[7] Lei *et al.* used melem single crystal nanorods as a photocatalyst with modulated charge potentials and dynamics.[8] Recently, Liu *et al.* improved the photocatalytic properties of carbon nitride for water splitting by attaching melem to Schiff base bonds.[9] In another report, a promotion in photocatalytic activity was obtained by construction of melem/g-C_3N_4 vermiculite hybrid photocatalyst for photo-degradation of tetracycline.[10] Lei *et al.* reported that H_2 evolution activity of melem derived g-C_3N_4 was 18 times higher than g-C_3N_4.[11] Melem was also utilized as a precursor for the preparation of rod-like g-C_3N_4/V_2O_5 heterostructure with enhanced sonophotocatalytic degradation for tetracycline antibiotics.[12] CO_2 cycloaddition into cyclic carbonates,[13] non-sacrificial photocatalytic H_2O_2 production,[3] water treatment,[14] simultaneous reductions of Cr(VI) and degradation of 5-sulfosalicylic acid,[15] are some of the catalytic applications of melem at various fields of sciences.

The main protocol of preparing melem is the annealing of cyanamide, dicyanamide, or melamine, which requires precise temperature control under an inert atmosphere such as N_2 or argon. Just recently, the synthesis approaches for molecular *s*-heptazines as well as their applications and properties have been reviewed by Audebert *et al.*[1b] Most of the reported methods do not lead to the preparation of pure monomer melem and are often mixed with its oligomers and polymerized derivatives,[16] meanwhile the possibility of forming triazine oligomers or oligomers between melem and triazine cannot be precluded.[5,16c] Complete polymerization of melamine at 500–550 °C leads to g-C_3N_4 and at 400–450 °C leads to melem-like derivatives,[17] mostly a mixture of different products requiring careful attention during isolation and purification.[5] Recently, Kessler and his colleague investigated the thermolysis of melamine, the formation of melem, and the formation of poly(triazine imide) from melem precursor *via* ionothermal as well as thermal condensation (conventional synthesis) as the back reaction of the melem condensation.[18]

The growing demands for employing melem in new applications besides the serious problems in preparing pure samples necessitate the development of a simple and operational scale-up method that does not have any acute and controlled conditions.

[a]*Catalysis Research Laboratory, Department of Chemistry, Faculty of Science, University of Birjand, Birjand, 97175-414, Iran. E-mail: rrezaeifard@birjand.ac.ir; rrezaeifard@gmail.com; mjafarpour@birjand.ac.ir*

[b]*Institute of Natural Sciences and Mathematics, Ural Federal University named after the B. N. Yeltsin, Ekaterinburg 620002, Russia*

† Electronic supplementary information (ESI) available: Experimental synthetic procedures and some characterization data. See DOI: 10.1039/d1ra07440g

It is well-known that the polycondensation mode of g-C_3N_4 and consequently the chemical and thermal stability as well as texture properties strongly depend on the nitrogen rich precursors (cyanamide, dicyandiamide, urea, and melamine) as well as annealing temperature.[19]

The interaction between the molecular precursors and/or intermediate compounds are critical factors.[17] Due to some drawbacks associated with the g-C_3N_4 such as low electronic conductivity, a high rate of photogenerated electron–hole pairs, a low surface area, poor visible-light absorption, low quantum yield, and low solubility in almost all of the traditional solvents,[20] it has been subjected to various acid treatments, to promote its properties and photochemical activity.[21] Various nanosheets with different properties and morphologies have been obtained depending on the precursor used, acid nature and concentration, as well as reaction temperature and time.[22] However, the oxidation products such as cyameluric or cyanuric acids (Scheme 1) under high reaction temperatures and times have been reported.[21c]

Inspired by the previous reports to prepare the acidified g-C_3N_4, we started with melamine to synthesize the g-C_3N_4 by calcining at 550 °C under air,[23] followed by the treatment with H_2SO_4. Nevertheless, we discovered that stirring the melamine-based g-C_3N_4 at concentrated H_2SO_4 (95–98%) at 80 °C for a limited time (1 h), afforded selectively monomer melem in high yield (Scheme 1). Following the intercalation, chemical exfoliation, and protonation of nitrogen atoms of the g-C_3N_4 sheets at concentrated H_2SO_4,[22,24] the bridging C–NH–C groups between *s*-heptazine units breaks which releases the triamino-*s*-heptazine (melem) molecules as monomer (Scheme S1†). Under these conditions the formation of oligomers was precluded because of the effective breaking of the bridging amino groups, however, the limited reaction time and moderate temperature prevented the tri-*s*-triazine ring-opening as well as the formation of the oxidation products such as cyameluric (or cyanuric) acids.[21c] Thus, we developed a facile and easy gram-scale synthesis of melem from acidic depolymerization of melamine-based g-C_3N_4 with no need for controlled conditions, and inert atmosphere. The air-stable white powder was insoluble in most common solvents (H_2O, C_2H_5OH, CH_3OH, DMF, CH_3CN, acetone, *etc.*) and only dissolved in DMSO with a very limited solubility exactly like that reported for the isolated pure monomer melem.[5,25] A new and distinctive rectangular prism morphology with an improved surface area was detected for the as-prepared melem,[5,8,26] which makes our study even more unique and novel.[5,8,27] It is well known that both morphology and specific surface area play important roles in affecting the photocatalytic activity of semiconductors.[22,28] Thus, our study not only provides a novel practical method for the preparation of nanostructured monomer melem, but also paves a new pathway for increasing its surface area. The chemical structure and purity of the as-prepared melem were verified by the combination of different techniques including FT-IR, ^{1}H and ^{13}C NMR, mass spectra, elemental analysis, XRD, XPS, DRS, and photoluminescence spectroscopy.

FT-IR spectrum of g-C_3N_4 and the as-prepared melem are depicted in Fig. 1. While the peaks at 803 and 796 cm^{-1} exhibited the vibrations of tri-*s*-triazine moieties in g-C_3N_4 and melem respectively, two intense bands at 1622 and 1471 cm^{-1}, consistent with those of monomer melem. The lack of obvious C–NH–C vibrations at around 1230 cm^{-1} featured the absence or negligible amount of dimelem or further melem-oligomers in the product.[29a,5,8] In the region of NH-stretching frequencies, a spectrum characteristic of amides is observed: three diffuse absorption bands (3415, 3360, and 3106 cm^{-1}) indicate the presence of strong intermolecular hydrogen bonds and strong interaction between the amino-groups and the ring.[29a] Inspection of the characteristic bands of melem presented in Fig. 1, no evidence for the formation of cyameluric acid or other oxidation products (Scheme 1) was detected.[29]

In the ^{13}C NMR spectrum (Fig. S1†), two signals at 165.8 and 156 ppm are assigned to carbon atoms adjacent to the amino groups and CN3 groups in heptazine rings, respectively.[1a,5] The ^{1}H NMR (Fig. S1†) showed a sharp signal at 7.4 ppm assigned to six protons of the terminal amino groups of melem along with two weak broad signals at ~8 ppm which can be attributed to the partial protonation of some nitrogens. The lack of the signal

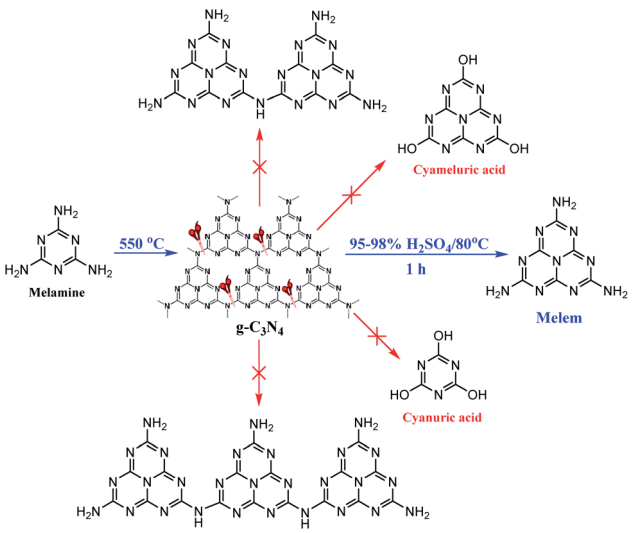

Scheme 1 The selective production of the monomer melem from melamine-based g-C_3N_4 presented in this work. Other molecules are possible decomposition and/or oxidation products of g-C_3N_4.

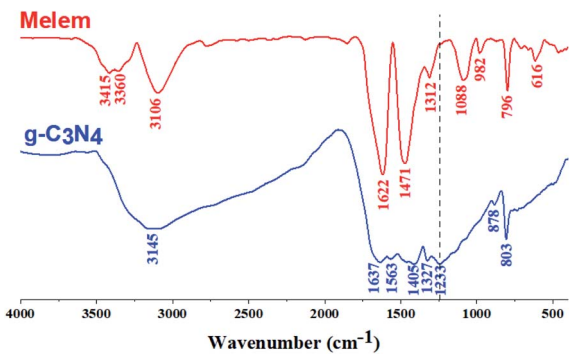

Fig. 1 FT-IR of the as-synthesized g-C_3N_4 and Melem.

at 149.37 ppm in ^{13}C NMR[29b] and a high-field signal at ^{1}H NMR (10.9 ppm or higher)[30] strongly confirmed that our method precludes the formation of cyameluric acid accompanied by the desired melem.

The mass spectrometry depicted in Fig. S2† shows that the bulk material contains almost entirely monomer melem evidenced by the main peak at m/z 218 pertinent to a single unit of melem and a very little peak at m/z 419 corresponding to dimelem and nothing of higher mass.[31] Also, no trace of the oxidation products was observed in mass spectra (m/z 129 and 221 for cyanuric and cyameluric acids, respectively).

The C/N atomic ratio is one of the most significant clues to prove the successful formation of melem. The ratio of 0.605 found for the produced melem is very close to the theoretical value in the monomer melem (C/N = 0.6).[5,8]

A substantial evidence for the exclusive formation of monomer melem was achieved by the XRD pattern. Fig. 2 shows XRD patterns of melem and its polymeric graphitic carbon nitride used in this work. A great match with literature was observed.[5] Two characteristic peaks of g-C_3N_4 at $2\theta = 13.28°$ (100) and 27.47° (002) related to the in-plane structural packing motif, and interlayer-stacking of aromatic systems respectively, significantly changed after treatment with 80 °C concentrated sulfuric acid for 1 h and showed strong evidence for the formation of the monomer melem.[5,8] The former peak (100) became pronounced and shifted to a lower angle of 12.52°, while the latter one (002) was shortened in the melem and shifted to the higher angle of $2\theta = 27.6°$ caused by decreased stacking distance between the melem inter-layers. More important is the emergence of a new intense peak at 6.16°, which is the unique characteristic of monomer melem,[5] while, other weak peaks located at about 19, 23, 25, 29 and, 31 are almost looked at in the XRD patterns of both monomer and oligomers.[5,8] No trace of cyameluric acid as the possible oxidation product was detected in the XRD pattern of the resulting product.[21c,30]

Next, XPS was used to identify the chemical environments of the product as shown in Fig. 3 and S3.† Only C, N, and trace amounts of O and S caused by the negligible remaining sulfuric acid and water can be detected (Fig. S3†). The C1s signals (Fig. 3 left) can be fitted into five components with binding energies of 284.5 eV, 285.18 eV, 287.78 eV, 288.58 eV, and 293.58 eV. The C signal at 284.5 eV is exclusively assigned to carbon atoms (C–C bonding) in a pure carbon environment, such as graphitic or amorphous carbons.[26,32] The signals at 285.16 and 287.78–288.3 eV attributed to graphitic carbon sp^2 C–C, and the sp^2 trigonal C–N bonding (*s*-triazine ring), respectively, characteristic of melem structure.[8,33] The advent of a high-energy satellite at 293.7 eV corresponds to the Π-electron delocalization in the heptazine system of melem.[27] The N 1s signals (Fig. 3 right) were deconvolved into five peaks. The signals with binding energies of 398.4, 400, and 401–404 eV are associated with the sp^2-hybridized nitrogen (C=N–C), tertiary nitrogen (N–$(C)_3$), and protonated amino groups (C–N–H) in melem, respectively.[33a,34] The emergence of (N–$(C)_3$) undoubtedly indicated the preservation of tri-*s*-triazine units (C_6N_7, basic part of melem molecule) during treatment with 80 °C concentrated acid. Thus, no significant changes in the carbon nitride heterocycles such as the oxidation transformation of terminal C–NH–C to C–OH–C and/or tri-*s*-triazine ring-opening reactions occurred.[21c,36] The advent of a satellite at high binding energy of 406 eV corresponds to the partial protonation of some nitrogens (N–H^+).[35]

The morphology of the as-synthesized product was determined by FESEM (Fig. 4A). The FESEM images clearly show microsized rectangular prisms with thickness ranging from ~50 to 350 nm, which was completely different with carbon nitride with the main nanosheets morphology.[37] To the best of our knowledge, this is the first report for such a morphology for melem,[8] that aroused our curiosity to assess its surface properties. The porosity of the samples was determined by N_2 physisorption experiments. The N_2 adsorption/desorption isotherms and pore size distributions of the as-prepared melem are given in Fig. 4B. The sample exhibited typical type IV isotherms with H3 hysteresis loop according to the IUPAC classification,[27] suggesting mesoporous structures with slit-shaped pores resulting from the aggregation of plate-like particles.[38] The BET specific surface area of the as-synthesized melem was found to be 19.54 $m^2\ g^{-1}$ which is about 3–4 folds larger than those reported for bulk melems as 5.63 $m^2\ g^{-1}$,[27] and 7.02 $m^2\ g^{-1}$,[12] as well as melem nanorods as 4.87 $m^2\ g^{-1}$,[8] obtained from the condensation of melamine. These results

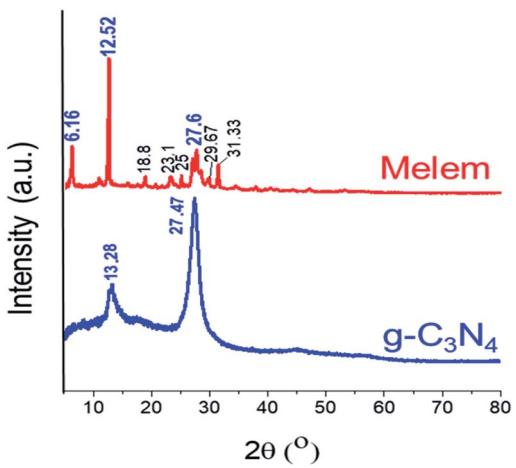

Fig. 2 XRD patterns of g-C_3N_4 and the as-synthesized melem.

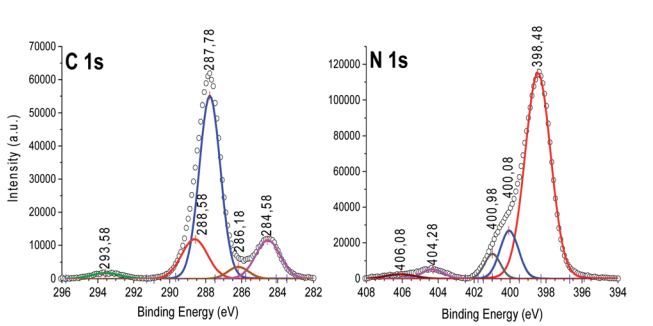

Fig. 3 XPS spectra of the as-prepared melem, left: C 1s and right: N 1s.

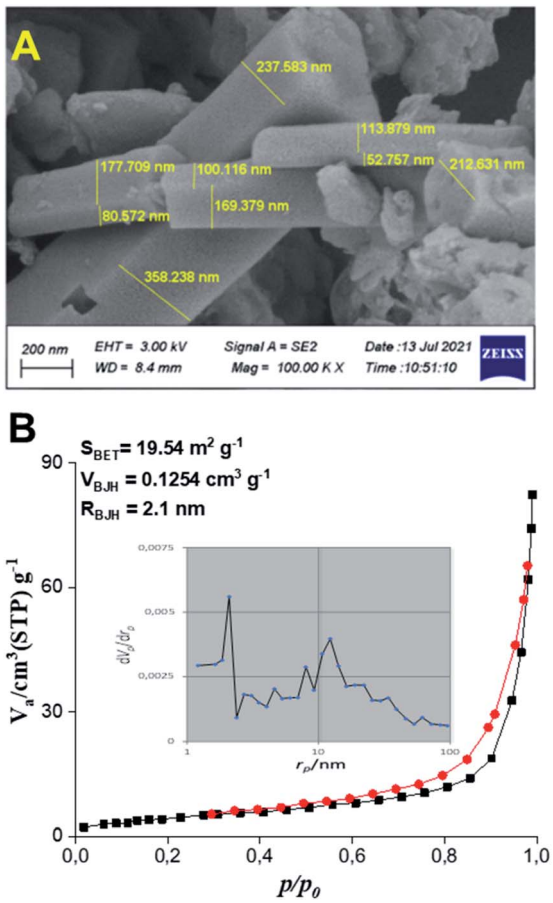

Fig. 4 (A) FESEM image and (B) BET N_2 adsorption/desorption isotherms of the as-synthesized melem.

clearly show the superiority of our easy-to-make melem over the other samples obtained by the traditional bottom-up design under quite controlled conditions.[5,8,27] The mesoporous nature of the as-synthesized melem was further supported by the pore-size distribution analysis depicted as an inset of isotherm (in Fig. 4B) indicating an average diameter of pore size at 2.1 nm.

The TG analysis of the as-synthesized melem exhibited three mass loss steps (Fig. S4†). At the first step, the sample lost about 10% of its weight at less than 200 °C caused by removing water and ethanol molecules absorbed during the elution process. The second one was begun at around 240 °C and continued to 500 °C with the evolution of ammonia and small amounts of HCN, attributed to the condensation polymerization of the monomer.

The third thermal decomposition was accelerated above 500 °C (with releasing HCN and C_2N_2),[6] rendering strong evidence for the absence of triazine derivatives (or lower) in the as-prepared product and once again ruled out the tri-*s*-triazine ring-opening reactions during the synthesis of melem in this work.[21c,39] The high thermal stability of the produced melem,[6] is comparable with the parent g-C_3N_4, making it more appropriate for comparative studies and applied goals that add further benefits to our sample.

Lastly, the optical properties of the sample were evaluated using UV-Vis diffuse reflectance spectroscopy (DRS). As shown in Fig. S5,† the absorption maximum wavelength of the resulting melem locates at 310 nm coincides with that reported in the literature.[5,40] The band edge of melem shifted to the lower wavelength (380 nm) compared to the polymer g-C_3N_4 (460 nm), caused by decreasing in Π-electron delocalization in the heptazine system of melem which stretches the band gap from 2.7 eV (polymer) to 3.45 eV (monomer melem) in excellent agreement with reported theoretical value for monomer melem (3.497 eV).[5,27] Further support for this claim was obtained by fluorescence spectra. Fig. 5 shows the comparative fluorescence spectra of the as-synthesized melem, under 355 nm light excitation. As shown in Fig. 5, it is found that the fluorescence emission of polymer g-C_3N_4 peaked at 476 nm,[40a] shifted to 412 nm in the melem coincide with Ricci report (415 nm).[41] In addition, the photoluminescence intensity of the resulting melem increased significantly compared to polymer g-C_3N_4 in broad agreement with literature indicating that the condensation of melem to g-C_3N_4 causes the weaker photoluminescence.[40a]

Finally, our formulation is very simple and robust with respect to processing conditions to overcome the potential scale-up problems to make it operational and amenable to scalability readily. As an example, a 5 fold semi-scaled-up procedure using 1.0 g g-C_3N_4 led to the isolation of the related pure monomer melem in 95% yield within 1 h.

In summary, we developed a novel operational protocol for easy gram scale preparation of air-stable monomer melem through a top-down synthesis design with no need for any control conditions and further purification. Our analyses ruled out the presence of the starting polymer as well as the formation of oligomers and oxidation products in the final product highlighting the selectivity of the method toward the monomer of melem. The distinctive nano rectangular prism morphology with desired surface area and thermal stability, as well as the appropriate photoluminescence property qualifies our synthesized melem for applied goals and makes it a promising

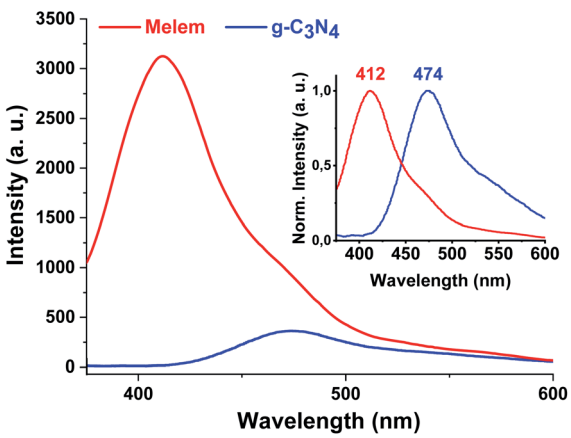

Fig. 5 Photoluminescence spectra of g-C_3N_4 and the as-synthesized melem under 355 nm light excitation.

alternative for catalysis and adsorption processes which is under investigation in our lab.

Conflicts of interest

There are no conflicts to declare.

Acknowledgements

We appreciate the Research Council of the University of Birjand for support of this work. The equipment of the Ural Center for Shared Use "Modern nanotechnology" Ural Federal University (Reg. NO. 2968) was used with the financial support of the Ministry of Science and Higher Education of the RF (Project NO. 075-15-2021-677).

Notes and references

1 (*a*) B. Jürgens, E. Irran, J. Senker, P. Kroll, H. Müller and W. Schnick, *J. Am. Chem. Soc.*, 2003, **125**, 10288–10300; (*b*) P. Audebert, E. Kroke, C. Posern and S. H. Lee, *Chem. Rev.*, 2021, **121**(4), 2515–2544.

2 C. Yang, K. Folens, G. Du Laing, F. Artizzu and R. Van Deun, *Adv. Funct. Mater.*, 2020, **30**(39), 2003656.

3 Z. Teng, W. Cai, S. Liu, C. Wang, Q. Zhang, S. Chenliang and T. Ohno, *Appl. Catal., B*, 2020, **271**, 118917.

4 H. B. Zheng, W. Chen, H. Gao, Y. Y. Wang, H. Y. Guo, S. Q. Guo, Z. L. Tang and J. Y. Zhang, *J. Mater. Chem. C*, 2017, **5**(41), 10746–10753.

5 V. W. H. Lau, M. B. Mesch, V. Duppel, V. Blum, J. Senker and B. V. Lotsch, *J. Am. Chem. Soc.*, 2015, **137**(3), 1064–1072.

6 H. Zheng, Z. Zhao, J. B. Phan, H. Ning, Q. Huang, R. Wang, J. Zhang and W. Chen, *ACS Appl. Mater. Interfaces*, 2019, **12**(2), 2145–2151.

7 D. Yang, L. Li, G. Xiao and S. Zhang, *Appl. Surf. Sci.*, 2020, **510**, 145345.

8 R. Lei, B. Du, X. Lai, J. Wu, Z. Zhang, S. Liu, R. Wu, X. Li, B. Song and J. Jian, *J. Mater. Chem. A*, 2019, **7**(21), 13234–13241.

9 H. Liu, M. Shen, P. Zhou, Z. Guo, X. Liu, W. Yang, M. Gao, M. Chen, H. Guan, N. P. Padture and S. Sun, *Nanoscale*, 2021, **13**(20), 9315–9321.

10 C. Huang, S. Zhang, M. Wang, H. Xu, M. Li, B. Song, G. Shao, H. Wang, H. Lu and R. Zhang, *Appl. Clay Sci.*, 2021, **213**, 106242.

11 L. Lei, W. Wang, Y. Shang, J. Li, A. K. Yadav, H. Wang, Q. Li and H. Fan, *Appl. Surf. Sci.*, 2021, 150384.

12 P. Mani, V. Vasudevan and N. Bernaurdshaw, *Chemosphere*, 2021, 132380.

13 H. Ding, Y. He, J. Ding, H. Wan and G. Guan, *ChemistrySelect*, 2021, **6**(12), 2951–2958.

14 S. Liu, H. Sun, K. O'Donnell, H. M. Ang, M. O. Tade and S. Wang, *J. Colloid Interface Sci.*, 2016, **464**, 10–17.

15 H. Lan, L. Li, H. Liu, X. An, F. Liu, C. Chen and J. Qu, *J. Colloid Interface Sci.*, 2017, **507**, 162–171.

16 (*a*) S. Lu, W. Zhou, M. Yang, G. Chen, W. Hong, D. Yu, Z. Zheng and X. Chen, *Polymer*, 2019, **182**, 121810; (*b*) E. Wirnhier, M. B. Mesch, J. Senker and W. Schnick, *Chem. - Eur. J.*, 2013, **19**(6), 2041–2049; (*c*) Y. Miyake, G. Seo, K. Matsuhashi, N. Takada and K. Kanai, *Mater. Adv.*, 2021, **2**, 6083–6093.

17 M. Majdoub, Z. Anfar and A. Amedlous, *ACS Nano*, 2020, **14**(10), 12390–12469.

18 F. K. Kessler and W. Schnick, *Z. Anorg. Allg. Chem.*, 2019, **645**(12), 857–862.

19 S. Patnaik, S. Martha and K. M. Parida, *RSC Adv.*, 2016, **6**, 46929–46951.

20 M. Mousavi, A. Habibi-Yangjeh and S. R. Pouran, *J. Mater. Sci.: Mater. Electron.*, 2018, **29**, 1719–1747.

21 (*a*) Z. Zhou, J. Wang, J. Yu, Y. Shen, Y. Li, A. Liu, S. Liu and Y. Zhang, *J. Am. Chem. Soc.*, 2015, **137**, 2179–2182; (*b*) J. Y. Song, H. J. Kang, J. C. Won, Y. H. Kim, Y. S. Jun and H. S. Jeong, *Mater. Horiz.*, 2019, **6**, 1726–1732; (*c*) H. -J. Kang, T. G. Lee, G. A. K. M Rafiqul Bari, H. -W. Seo, J.-W. Park, H. J. Hwang, B.-H. An, N. Suzuki, A. Fujishima, J.-H. Kim, H. K. Shon and Y.-S. Jun, *Catal*, 2021, **11**, 37.

22 (*a*) K. Wang, S. Song, Q. Zhang, Y. Jin and Q. Zhang, *Chem. Commun.*, 2019, **55**, 7414–7417; (*b*) R. C. Pawar, S. Kang, J. H. Park, J. H. Kim, S. Ahn and C. S. Lee, *Sci. Rep.*, 2016, **6**, 1–14; (*c*) X. Du, G. Zou, Z. Wang and X. Wang, *Nanoscale*, 2015, **7**, 8701–8706; (*d*) L. Shi, W. Ding, S. Yang, Z. He and S. Liu, *J. Hazard. Mater.*, 2018, **347**, 431–441; (*e*) M. Cao, J. Zuo, Y. Huang and Z. Liu, *J. Mater. Sci. Mater. Electron.*, 2020, **31**, 2022–2029; (*f*) J. Tong, L. Zhang, F. Li, K. Wang, L. Han and S. Cao, *RSC Adv.*, 2015, **5**, 88149–88153; (*g*) J. H. Lee, M. J. Park, S. J. Yoo, J. H. Jang, H. J. Kim, S. W. Nam, C. W. Yoon and J. Y. Kim, *Nanoscale*, 2015, **7**, 10334–10339; (*h*) Y. Liu, X. Zhang, J. Wan and P. Yang, *RSC Adv.*, 2016, **6**, 112581–112588; (*i*) L. R. Zou, G. F. Huang, D. F. Li, J. H. Liu, A. L. Pan and W. Q. Huang, *RSC Adv.*, 2016, **6**, 86688–86694; (*j*) S. Cheng, X. Meng, N. Shang, S. Gao, C. Feng, C. Wang and Z. Wang, *New J. Chem.*, 2018, **42**, 1771–1778.

23 S. Liu, S. Wang, Y. Jiang, Z. Zhao, G. Jiang and Z. Sun, *Chem. Eng. J.*, 2019, **373**, 572–579.

24 X. Yang, F. Qian, G. Zou, M. Li, J. Lu, Y. Li and M. Bao, *Appl. Catal., B*, 2016, **193**, 22–35.

25 Y. Wang, N. Wu, C. Liu, M. K. Albolkany, M. Wang, Y. Wang, S. Arooj, W. Zhang and B. Liu, *Mater. Horiz.*, 2020, **7**(1), 149–156.

26 H. Piao and N. S. Mcintyre, *Surf. Interface Anal.*, 2002, **33**(7), 591–594.

27 N. Liu, T. Li, Z. Zhao, J. Liu, X. Luo, X. Yuan, K. Luo, J. He, D. Yu and Y. Zhao, *ACS omega*, 2020, **5**(21), 12557–12567.

28 (*a*) Z. Deng, M. Chen, G. Gu and L. Wu, *J. Phys. Chem. B*, 2008, **112**(1), 16–22; (*b*) H. Li, Z. Bian, J. Zhu, D. Zhang, G. Li, Y. Huo, H. Li and Y. Lu, *J. Am. Chem. Soc.*, 2007, **129**, 8406–8407.

29 (*a*) A. I. Finkelshtein and N. V. Spiridonova, *Russ. Chem. Rev.*, 1964, **33**(7), 400–405; (*b*) K. Kailasam, J. Schmidt, H. Bildirir, G. Zhang, S. Blechert, X. Wang and A. Thomas, *Macromol. Rapid Commun.*, 2013, **34**, 1008–1013.

30 L. Seyfarth, J. Sehnert, N. E. A. El-Gamel, W. Milius, E. Kroke, J. Breu and J. Senker, *J. Mol. Struct.*, 2008, **889**, 217–228.

31 D. Fischer, K. Schwinghammer, C. Sondermann, V. W. Lau, J. Mannhart and B. V. Lotsch, *Appl. Surf. Sci.*, 2015, **349**, 353–360.
32 J. S. Zhang, M. W. Zhang, G. G. Zhang and X. C. Wang, *ACS Catal.*, 2012, **2**, 940–948.
33 (*a*) A. Thomas, A. Fischer, F. Goettmann, M. Antonietti, J. O. Müller, R. Schlögl and J. M. Carlsson, *J. Mater. Chem.*, 2008, **18**(41), 4893–4908; (*b*) Y. H. Cheng, X. L. Qiao, J. G. Chen, Y. P. Wu, C. S. Xie, S. B. Muo, Y. B. Sun and B. K. Tay, *Appl. Phys. A*, 2002, **74**(2), 225–231.
34 (*a*) X. Weng, Q. Zeng, Y. Zhang, F. Dong and Z. Wu, *ACS Sustainable Chem. Eng.*, 2016, **4**(8), 4314–4320; (*b*) G. Yan, X. Feng, L. Xiao, W. Xi, H. Tan, H. Shi, Y. Wang and Y. Li, *Dalton Trans.*, 2017, **46**(46), 16019–16024.
35 A. J. Beck, J. D. Whittle, N. A. Bullett, P. Eves, S. Mac Neil, S. L. McArthur and A. G. Shard, *Plasma Processes Polym.*, 2005, **2**(8), 641–649.
36 T. S. Miller, A. B. Jorge, T. M. Suter, A. Sella and F. Cora, *Phys. Chem. Chem. Phys.*, 2017, **19**, 15613–15638.
37 (*a*) Z. Teng, N. Yang, H. Lv, S. Wang, M. Hu, C. Wang, D. Wang and G. Wang, *Chem*, 2019, **5**, 664–680; (*b*) F. He, Z. Wang, Y. Li, S. Peng and B. Liu, *Appl. Catal., B*, 2020, **269**, 118828.
38 K. A. Cychosz, R. Guillet-Nicolas, J. García-Martínez and M. Thommes, *Chem. Soc. Rev.*, 2017, **46**(2), 389–414.
39 E. Horvath-Bordon, E. Kroke, I. Svoboda, H. Fueß, R. Riedel, S. Neeraj and A. K. Cheetham, *Dalton Trans.*, 2004, 3900–3908.
40 (*a*) J. Wen, R. Li, R. Lu and A. Yu, *Chem.–Asian J.*, 2018, **13**(8), 1060–1066; (*b*) S. Chu, C. Wang, J. Feng, Y. Wang and Z. Zou, *Int. J. Hydrogen Energy*, 2014, **39**(25), 13519–13526.
41 L. Stagi, D. Chiriu, C. M. Carbonaro, R. Corpino and P. C. Ricci, *Diamond Relat. Mater.*, 2016, **68**, 84–92.